Low-frequency resonant magnetoelectric effects in a planar heterostructure of ferromagnetic yttrium iron garnet film and piezoelectric quartz

D.A. Burdin¹, D.V. Chashin¹, N.A. Ekonomov¹, P. Zhou², G. Srinivasan³, Y.K. Fetisov¹

¹MIREA – Russian Technological University, Moscow 119454, Russia

E-mail: <u>fetisov@mirea.ru</u> (Y.K. Fetisov)

Abstract

Low-frequency resonant magnetoelectric (ME) effects in a planar heterostructure containing a 50 µm thick single-crystal film of yttrium iron garnet (YIG) and a crystalline quartz platelet were studied. The ME effects in the mechanically coupled composite arise due to a combination of magnetostriction of the YIG film and the piezoelectric effect in quartz. The effects manifest as mutual transformation of ac magnetic and electric fields. When the layered composite was excited by an ac magnetic field (direct ME effect) at a planar acoustic resonance frequency of 128 kHz, the ME field conversion coefficient was 8.8 V/(Oe·cm). When excited by an ac electric field (converse effect), the ME conversion coefficient was 0.32 G/(V/cm). Nonlinear ME effects caused by the nonlinear magnetostriction of the YIG film were observed as frequency doubling upon excitation of the direct ME effect by a magnetic field at a frequency equal to half the resonant frequency, as well as at the converse ME effect upon excitation by an electric field at the frequency of the resonance of the structure. In spite of weak magnetostriction for YIG, the resonant ME effects in the YIG-quartz composite are comparable in magnitude to the effects in composites with high magnetostriction materials, show high quality factor of Q~2200 and are observed in weak magnetic fields $H\sim0.60$ Oe. These results demonstrate the potential for YIG filmquartz composites application in electronic devices.

Keywords: magnetoelectric effect, composite heterostructure, YIG film, magnetostriction, quartz, piezoelectricity, harmonics generation

1. Introduction

Magnetoelectric (ME) effects in composite heterostructures containing ferromagnetic (FM) and piezoelectric (PE) layers manifest themselves as a change in the electric polarization P of the

²School of Materials Science and Engineering, Hubei University, Wuhan 430062, China

³Physics Department, Oakland University, Rochester, MI 48309, United States of America

structure under the action of a magnetic field H (direct effect) or a change in the magnetization M of the structure under the action of an electric field E (converse effect) [1]. The effects arise as a result of a combination of magnetostriction of the FM layer and piezoelectricity of the PE layer in the mechanically coupled layers [2]. Under the direct ME effect, the field H results in magnetostrictive deformation of the FM layer and this deformation is transmitted through the interface to the PE layer that generates an electrical voltage due to piezoelectric effect. Under the converse ME effect, the field E leads to deformation of the PE layer and this deformation when transferred to the FM layer leads to a change in its magnetization due to the inverse magnetostriction (Villari effect). Interest in the study of ME effects in heterostructures is primarily due the prospects for a variety of applications, including highly sensitive magnetic field sensors, electrically tunable electronic devices, energy harvesting devices, information storage and processing devices [3-5].

The strength of the direct ME effect is measured by the coefficient $\alpha_E = \delta E/\delta H$, and the magnitude of the converse effect by the coefficient $\alpha_B = \delta B/\delta E$, where δE is the change in the electric field in the PE layer caused by the change in the magnetic field δH , δB is the change in the magnetic induction in the FM layer caused by the change in the electric field δE . To enhance the efficiency of fields conversion, FM layers of structures are made of materials with high magnetostriction λ (metals Ni, Co, alloys FeCo, Terfenol-D, amorphous alloys, ferrites), and PE layers are made of materials with large piezoelectric modulus d (ceramics of PZT type, crystals of PMN-PT type, AlN, lithium niobate, languatate, quartz, piezopolymers of the PVDF type) [5, 6]. In addition, when the frequency of the magnetic or electric field coincides with the frequencies of acoustic vibrations of ME structures, the coefficients increase by two orders of magnitude due to the resonant increase in deformations [7]. To date, ME coefficients of $\alpha_E \sim 1-10^3$ V/(Oe·cm) and $\alpha_B \sim 0.1-5$ G/(V/cm) have been achieved in layered heterostructures made of various materials, which is several orders of magnitude higher than the ME coefficients in single-phase multiferroics and bulk composite materials [5].

For applications, it is of interest to study ME effects in heterostructures with FM layers of yttrium iron garnet (YIG) ferrite, which has a number of unique properties and is therefore widely used in microwave electronics, magneto-optics, and acousto-electronics [8,9]. YIG is ferrimagnetic with low acoustic losses, and is a good dielectric with the lowest magnetic losses in the microwave range. Bulk single crystals of YIG are prepared by melt growth and YIG films with thicknesses from fractions of a micron to ~100 microns by liquid-phase epitaxy or by gas-phase and laser deposition on gadolinium gallium garnet (GGG) and semiconductor substrates. [10].

It is shown that YIG single crystals themselves exhibit a weak ME effect of $\alpha_E \sim 2$ mV/(Oe·cm), induced by a dc electric field $E\sim7.5$ kV/cm applied to the crystal, due to the crystal

symmetry breaking [11,12]. The ME effect up to $\alpha_E \sim 12$ mV/(Oe·cm) was reported for particulate composites based on ferroelectric YFeO₃ and YIG powders [13]. The ME effect up to $\alpha_E \sim 20$ mV/(Oe·cm) was measured in composites based on powders of piezoelectric lithium sodium potassium niobate (KLNN) and YIG [14].

In planar heterostructures with YIG and various PE, the converse ME effect was studied extensively. A change in the orientation of magnetization in the structure of a YIG film – lead magnesium niobate - lead zirconate titanate (PMN-PZT) was demonstrated when an electric field is applied to the piezoelectric layer [15]. The tuning of the ferromagnetic resonance in the YIG - lead magnesium niobate - lead titanate (PMN-PT) structure under the action of an electric field applied to the piezoelectric layer of the structure was reported [16]. The tuning of frequency of thickness acoustic modes in the ZnO – YIG structure on a GGG substrate under the action of external magnetic field was observed [17].

To our knowledge, there is only one report [18] where the low-frequency ME effect was studied in layered composites with YIG and PMN-PT. In this work polycrystalline, single-crystal, and epitaxial YIG layers with thicknesses from 10 μ m to 58 μ m were used. For direct ME effect in a composite with a thick YIG film, an ME conversion coefficient of $\alpha_E = 250$ mV/(Oe·cm) was obtained at a frequency of 100 Hz.

Here we report on a detailed investigation of linear and nonlinear resonant ME effects in a heterostructure containing a layered composite of epitaxial YIG film and piezoelectric quartz. Single-crystal quartz was chosen as a piezoelectric material, since it has a high acoustic quality factor, which makes it possible to achieve large deformations at the acoustic resonance frequency and facilitates the observation of nonlinear ME effects. The second part of the report is devoted to the description of the structure under study and measurement techniques. The third and forth parts present the results of studies of direct linear and nonlinear ME effects. The fifth and six parts contain a description of the converse linear and nonlinear ME effects in the structure. This is followed by a discussion and explanation of the obtained data. We conclude with a summary of the main results of this work.

2. Structure and experimental techniques

The composite under study is shown schematically in Fig. 1. It contains a film of yttrium iron garnet ferrite of composition $Y_3Fe_5O_{12}$ (YIG) and a quartz layer. The YIG film had a length L=22 mm, a width of 3 mm and a thickness of a_m =50 μ m. The single-crystal YIG film was grown by the liquid-phase epitaxy on both sides of a 500 μ m thick gallium gadolinium garnet $Ga_3Gd_5O_{12}$ (GGG) substrate with (111) orientation. Then the film on one side of the substrate was removed and the

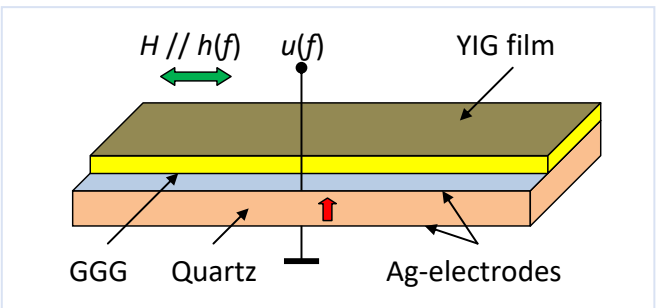


Fig.1. Schematic representation of a planar composite heterostructure YIG film on a GGG-quartz substrate. The arrows indicate directions of the excitation field h, and dc magnetic H and electric E fields.

thickness of the substrate was reduced to a_s =310 µm. The saturation magnetization of the film, measured with a vibrating sample magnetometer, was $4\pi M_{\rm S}\approx 1750$ G, the saturation magnetostriction measured by the tensometric method was $\lambda_{\rm S}\approx 2.1\cdot 10^{-6}$ for $H_{\rm S}\approx 80$ Oe, the FMR linewidth at a frequency of 9 GHz was $\Delta H\approx 0.8$ Oe. The single-crystal quartz plate had a length L=22 mm, a width of

4 mm, and a thickness of $a_p=1$ mm. The long axis of the plate coincided with the optical axis of the quartz. The piezomodulus and the relative permittivity for quartz were equal to $d_{11}=2.4$ nC/N and $\epsilon=6.8$, recpectively [19]. Ag-electrodes, 1 µm thick, were deposited on both surfaces of the quartz plate by magnetron sputtering. The capacitance of the resulting capacitor, measured at a frequency of 10 kHz, was $C \approx 5$ pF. The YIG film on the GGG substrate was bonded onto the quartz plate from the GGG substrate side using a cyanoacrylate epoxy. The adhesive layer, ~5 µm thick, effectively transmitted deformations through the interface. The structure was fixed in the central part with the help of two conductors, 0.1 mm in diameter, soldered to Ag-electrodes, which ensured effective excitation of the fundamental mode of longitudinal vibrations of the structure.

When studying the direct ME effect, the composite was placed between Helmholtz coils with a diameter of 15 cm, which were powered by a stabilized TDK-Lambda GENH600-1.3 source. The coils created a dc magnetic field H=0-100 Oe directed along the long axis of the structure. An excitation magnetic field with a frequency of f = 10 Hz – 200 kHz and an amplitude up to h = 2.5 Oe was created using a coil enclosing the structure and connected to an Agilent model 33210A generator. A coil of 20 mm in length and 20 mm in diameter contained 60 turns of wire, had an active resistance of 1.35 Ω and an inductance of 70 μ H. The excitation magnetic field h was directed parallel to the dc field h. The voltage generated by the composite was measured using a Stanford Research SR844 lock-in amplifier with an input impedance of 10 M Ω . The voltage waveform and voltage frequency spectra were recorded using a Tektronix TDS 3032B oscilloscope. The dependences of the ME voltage u on the frequency f and the amplitude h of the excitation field and the bias field H were measured.

When studying the converse ME effect, a harmonic electric voltage $U\cos(2\pi ft)$ with an amplitude U up to 10 V from the generator was applied to the quartz electrodes, and the change in induction δB in the FM layer of the structure was recorded using the same coil. The dc bias field was measured with a LakeShore 421 Gaussmeter with an accuracy of 0.1 Oe. The ac excitation field

was measured by the current through the coil calibrated at a frequency of 100 Hz. The measuring setup operated in automatic mode under the control of a specialized LabView program.

3. Linear direct ME effect

At first, the characteristics of the direct linear ME effect in the composite were measured when it was excited with an ac magnetic field h. Figure 2 shows typical frequency dependence of the amplitude of the voltage u(f) generated in the composite for h = 0.04 Oe and H = 10 Oe. Near the resonant frequency $f_d = 128.08$ kHz, a peak is seen with an amplitude $u_1 \approx 35$ mV and a quality

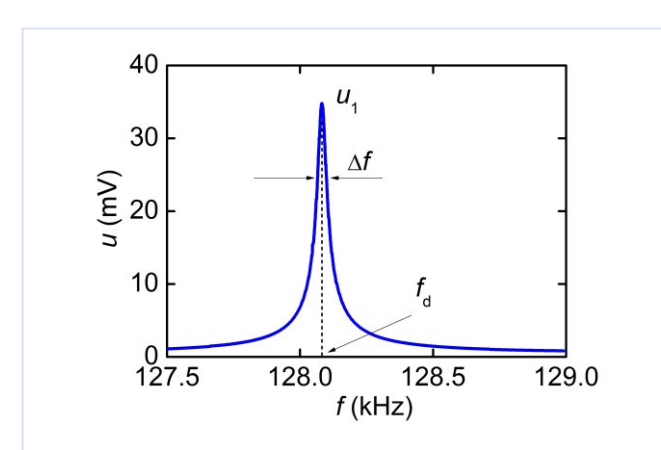


Fig. 2. Frequency f dependence of the voltage u due to direct ME effect for the YIG - quartz composite at H=10 Oe and h=0.04 Oe.

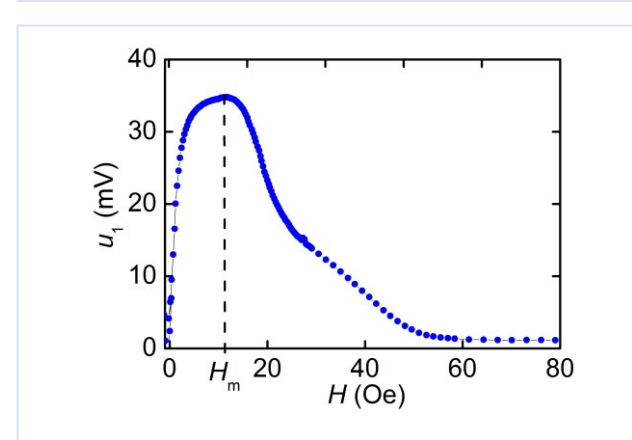


Fig. 3. Dependence of the ME voltage u_1 at the resonant frequency on the bias field H for the YIG - quartz layered structure.

factor of $Q_d = f_d/\Delta f \approx 2135$, where $\Delta f \approx 60$ Hz is the line width at half power. The frequency at the peak in the voltage corresponds to the lowest mode of longitudinal acoustic oscillations of the structure. In the case of the direct ME effect, the magnitude of the direct electromagnetic pickup did not exceed ~ 0.5 mV and was much less than the magnitude of the ME voltage at the resonant frequency.

Figure 3 shows the dependence of the ME voltage u_1 at the resonant frequency f_d on the bias field H for h=0.04 Oe. The dependence is a typical for the direct ME effect: the voltage initially increases approximately linearly with increasing H, reaches a maximum in the field region $H_m \approx 10$ -12 Oe, and then gradually drops to zero in fields above 60 Oe. The voltage drops rapidly in the field range of \sim 15–23 Oe and falls more slowly in the field range of 25–50 Oe. The hysteresis for this dependence was less than 0.3 Oe. The presence

of linear segments in the dependence $u_1(H)$ is unusual for structures with FM layers made of highly magnetostrictive materials. Note that the resonant frequency f_d changed by no more than ~10 Hz as the field H is increased, reaching a minimum at the field H_m , which indicates a small ΔY -effect in the YIG film compared to other magnetostrictive materials [20].

4. Nonlinear direct ME effect

Next, we consider the nonlinear ME effect and the related frequency doubling observed with an increase in the amplitude h of the excitation magnetic field. The composite structure was excited by

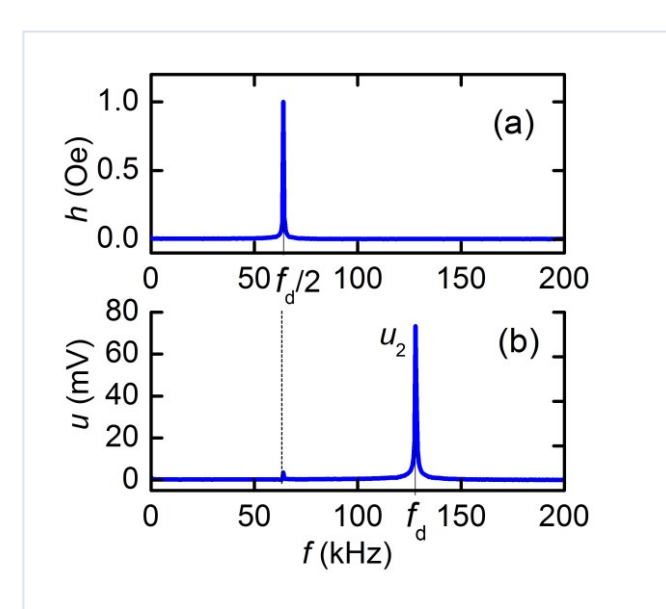


Fig. 4. Frequency spectra: (a) of the excitation magnetic field and (b) of the generated ME voltage at h=1 Oe and H=0 for the YIG- quartz structure at direct nonlinear ME effect.

a harmonic field with an amplitude h = 0–2.5 Oe and at a frequency $f_{\rm ex}$ equal to half of the resonant frequency of the structure, $f_{\rm ex} = f_{\rm d}/2$. The frequency spectrum of the generated ME voltage was recorded. As an example, Fig.4a shows the frequency spectrum of the excitation field h(f) and the frequency spectrum of u(f) for h=1 Oe in the absence of a bias field, H=0 Oe. It can be seen that the voltage spectrum contains a weak component of the frequency $f_{\rm d}/2$ due to direct electromagnetic pickup and a peak with an amplitude $u_2 \approx 73$ mV at $f_{\rm d}$, which is equal to the resonant frequency of the structure.

Figure 5 shows dependence of the amplitude of the second harmonic u_2 on the bias field H for h=2.5 Oe. Its maximum value is u_2 ≈456 mV at H=0 and it drops almost to zero in the field range H ~ 6-10 Oe. However, in the fields region of H~17-180 Oe there is a local maximum of the second harmonic, and in the region of H= 30-50 Oe there is a second weaker and wider local maximum. The amplitude of the first local maximum is ~4 times smaller than the amplitude of the maximum at H=0. The measurements showed (see Fig. 6) that the amplitude of the ME voltage with doubled frequency depends quadratically on the amplitude of h. Similar measurements were also carried out

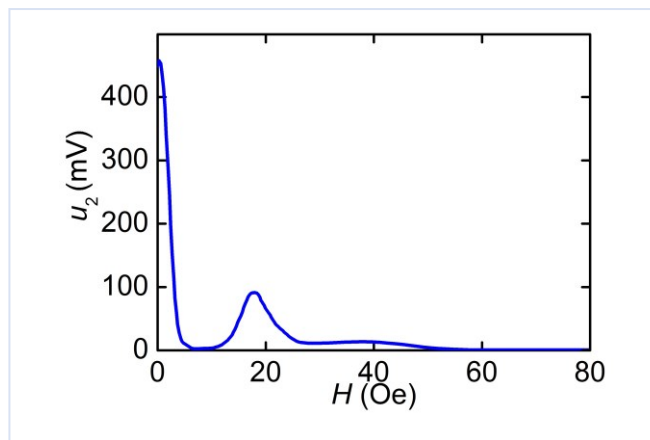


Fig. 5. Dependence of the ME voltage second harmonic amplitude u_2 the on the bias field H at h=2.5 Oe for the YIG-quartz structure at direct nonlinear ME effect.

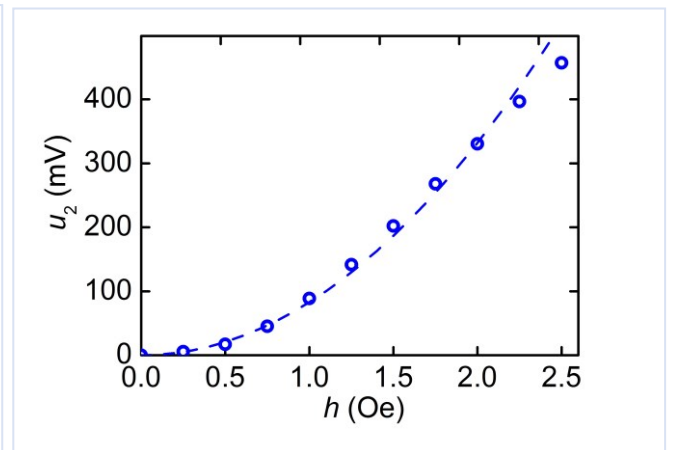


Fig. 6. Dependence of the ME voltage second harmonic amplitude u_2 on the excitation field h at H=0 for the YIG-quartz structure at direct nonlinear ME effect. The dashed line is a quadratic approximation.

for the nonlinear ME effect for h=0-2.5 Oe and excitation frequency equal to the acoustic resonance frequency of the structure $f_{\rm ex} = f_{\rm d}$. The frequency spectrum of the generated voltage was recorded near the frequency $f \sim 2f_{\rm d}$. In this case, a nonlinear ME effect of frequency doubling was also observed. The voltage frequency spectrum at H=0 and h = 1 Oe contained a harmonic with a doubled frequency and an amplitude of u_2 ~1.2 mV, i.e. by a factor of 60 smaller when the structure was excited at half frequency.

5. Linear converse ME effect

The nature of converse linear ME effect in the sample involved measurements when it was excited by an ac electric field. Figure 7 shows typical frequency dependences of the voltage v(f)

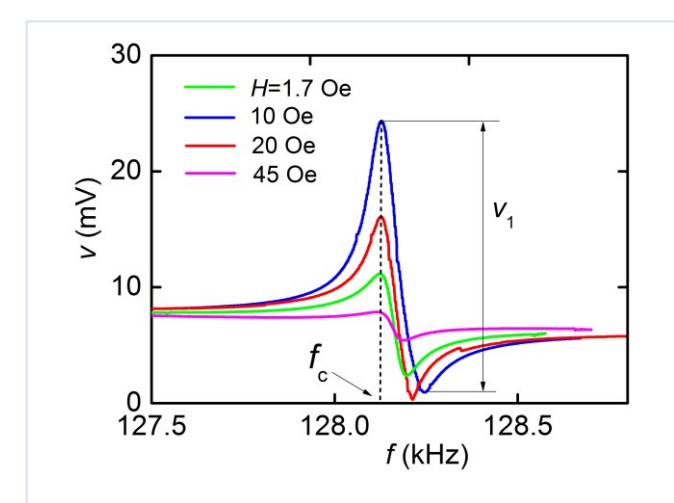


Fig. 7. Dependence of the converse ME voltage v on the frequency f of the excitation field at e=100 V/cm for different H for the YIG-quartz composite.

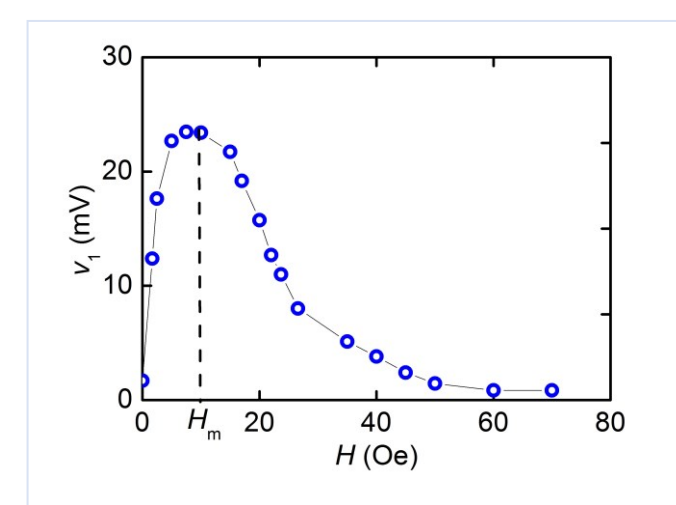


Fig. 8. Dependence of the voltage v_1 on the bias field H for e=100 V/cm applied at the resonant frequency for the YIG-quartz structure.

generated in the measuring coil for the field amplitude e=100 V/cm and for a series of bias fields H. For the converse ME effect the resonant frequency was $f_c=128.128$ kHz and also weakly depended on the dc field H. The asymmetric shape of the resonance profiles in 7 is due to the presence electromagnetic pickup ($v_{\text{ind}} \approx 7 \text{ mV}$ at e=100V/cm), which interferes with the ME signal. From the data in Fig.7, it was possible to extract the frequency dependence of the voltage generated in the measuring coil only due to the converse ME effect. For the Lorentzian shape of the ME voltage line, its amplitude is equal to the difference between the maximum and minimum voltages on each curve $v_1 = v_{\text{max}} - v_{\text{min}}$ (shown only for the field H=10 Oe). The quality factor of the resonance for the converse ME effect, defined as $Q_c = f_c / \Delta f$, where $2\Delta f \approx 116$ Hz is the frequency difference between the maximum and minimum points of the curve, was $Q_c \approx$ 2210.

Figure 8 shows the dependence of the voltage v_1 from the measuring coil on the dc field H, plotted using the data of Fig. 7. The dependence has qualitatively the same form as the dependence in Fig. 3 for the direct ME effect. The voltage first increases with increasing H, reaches a maximum in approximately the same field $H_{\rm m}\approx 10$ Oe, and then tends to zero as the YIG film is saturated. The number of points in Fig. 8 for the converse ME effect is less than in Fig. 3 for the direct ME effect, but on the descending section of the profile, two linear sections with different slopes are also distinguishable.

6. Nonlinear converse ME effect

Next, we investigated the frequency doubling due to the nonlinear converse ME effect observed upon an increase in the amplitude e of the excitation electric field. The composite was excited by a harmonic field with an amplitude e = 0–100 V/cm and a frequency f_c , equal to the resonance frequency of the structure, and the frequency spectrum of the voltage generated by the measuring coil was recorded. As an example, Fig. 9 shows the frequency spectra of the excitation field e(f) and the voltage spectrum v(f) generated by the ME coil at e=100 V/cm and the bias field H=20 Oe. It can be seen that the voltage frequency spectrum contains a harmonic v_1 with the frequency of excitation field and a second harmonic v_2 with a frequency of $2f_c$ and an amplitude of 1.83 mV.

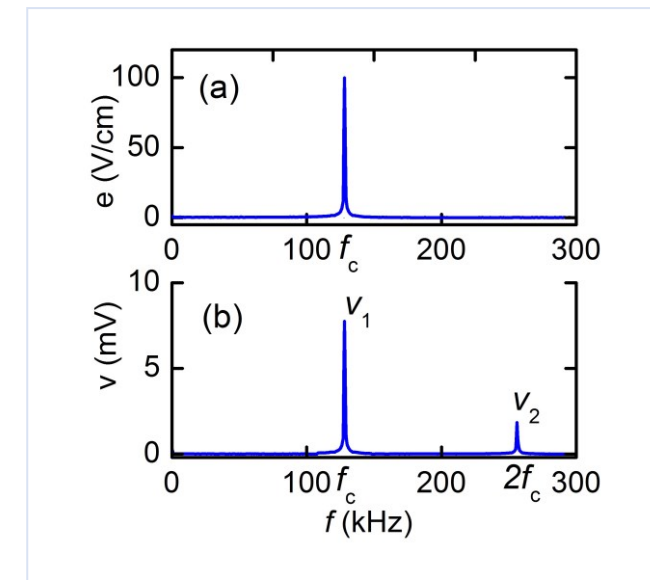


Fig. 9. Frequency spectrum of the excitation electric field and voltage from the coil at H=20 Oe and e=100 V/cm for the YIG-quartz structure at converse nonlinear ME effect.

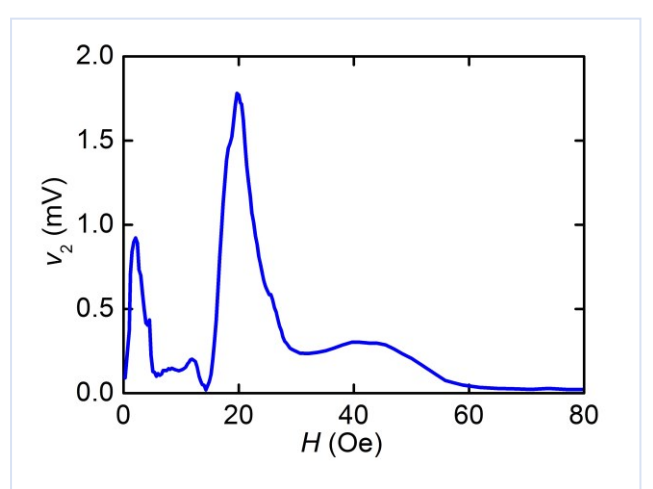


Fig. 10. Dependence of the voltage v_2 from the coil on the field H when excited the YIG-quartz structure at the resonance frequency by the field e=100 V/cm at converse nonlinear ME effect.

Figure 10 shows the dependence of the amplitude v_2 of the second harmonic on the bias field H for e=100 V/cm. It can be seen that the amplitude of the second harmonic has three maxima as the field increases: in a field of ~2 Oe, in a field of ~20 Oe, and in a field of ~40 Oe, and then drops monotonically and vanishes for H > 60 Oe. We emphasize that in the case of the converse nonlinear

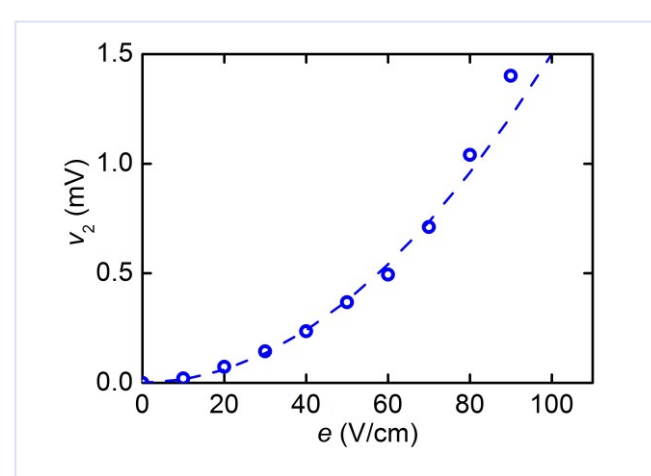


Fig. 11. Dependence of the voltage of the second harmonic v_2 from the coil on the amplitude of the field e at H=20 Oe for the YIG-quartz structure at converse non-linear ME effect. The dashed line is a quadratic approximation.

ME effect, the amplitude of the second harmonic is zero at H=0, in contrast to the direct nonlinear ME effect, where it is maximum in the absence of a field. Figure. 11 demonstrates the quadratic dependence of the amplitude of the second harmonic on the excitation field e for the converse nonlinear ME effect.

When the converse ME effect was studied for an excitation field at a frequency $f_c/2$ equal to half the resonant frequency, no voltage generation with a doubled frequency at the resonant frequency f_c was observed.

7. Discussion

First, we estimated the acoustic resonance frequency of a three-layer structure (YIG film, GGG substrate, and quartz) using the formula for the frequency of the fundamental mode of longitudinal vibrations of a free rod [21].

$$f_0 = \frac{1}{2L} \sqrt{\frac{Y}{\rho}} \,. \tag{1}$$

Here L is the length of the structure, $Y = (Y_m a_m + Y_s a_s + Y_p a_p)/a$, $\rho = (\rho_m a_m + \rho_s a_s + \rho_m a_m)/a$ are the effective Young's modulus and the effective density of the structure, respectively, $a = a_m + a_s + a_p$ is the total thickness of the structure. The contribution of the adhesive layer to the estimate can be ignored, because its thickness is more than two orders of magnitude less than the total thickness of the structure. Using the known parameters of the structure layers (YIG film: $a_m = 50 \, \mu m$, $Y_m = 20 \cdot 10^{10} \, \text{Pa}$, $\rho_m = 5.17 \cdot 10^3 \, \text{kg/m}^3$; GGG substrate: $a_s = 315 \, \mu m$, $Y_s = 20 \cdot 10^{10} \, \text{Pa}$, $\rho_s = 7.08 \cdot 10^3 \, \text{kg/m}^3$; quartz: $a_p = 1 \, \text{mm}$, $Y_p = 8 \cdot 10^{10} \, \text{Pa}$, $\rho_p = 2.65 \cdot 10^3 \, \text{kg/m}^3$), we obtained a resonance frequency of $f_0 \approx 131 \, \text{kHz}$. The calculated frequency agrees well with the measured resonant frequencies for the direct f_d and converse f_c ME effects.

Note the high quality factor of the acoustic resonances for both direct and converse ME effects $Q_d \approx Q_c \approx 2200$, which is typical for composites with layers of single-crystal materials [22, 23].

For the linear direct ME effect, the maximum value of the ME coefficient in the described YIG-quartz heterostructure at a bias field of $H_{\rm m}$ =12 Oe, as can be estimated using the data in Figs. 2 and 3, is $\alpha_E = u/(a_3h) \approx 8.8$ V/(Oe cm). The obtained ME coefficient is comparable to the coefficients

for structures with FM layers of Ni, permendur, and other highly magnetostrictive materials, and is achieved in weak magnetic fields, as in composites with Metglas alloy [3, 24]. In the case of the direct ME effect, the shape of the dependence $u_1(H)$ of ME voltage on the bias field (see Fig. 3) is determined by the field dependence of the magnetostriction of the FM layer $\lambda(H)$ [20, 25]

$$u_1(H) \sim QA \frac{d_{31}}{\varepsilon} \lambda^{(1)}(H). \tag{2}$$

In Eq.(2) Q is the quality factor of the structure, A is a constant depending only on the dimensions and mechanical parameters of the layers, $\lambda^{(1)}(H) = \partial \lambda / \partial H|_H$ is a linear piezomagnetic coefficient, $\lambda(H)$ is the dependence of the magnetostriction of the FM layer on the bias field H. As can be seen from Eq.(2), the amplitude of the ME voltage in each field differs from the piezomagnetic coefficient $\lambda^{(1)}$ only by the coefficient $K = QA(d_{31}/\varepsilon)$. This circumstance makes it possible to calculate the field dependence of the magnetostriction of the FM layer using the shape of the dependence $u_1(H)$ by means of integration

$$\lambda(H) = \frac{1}{K} \int_{0}^{H} u_1(H) dH. \tag{3}$$

The field dependence $\lambda(H)$ of the magnetostriction of the YIG film found by this method is shown in Fig. 12a with a solid line. To calibrate the absolute value of magnetostriction, the dependence $\lambda(H)$ was also measured using a strain gauge glued to the film surface [27] and shown

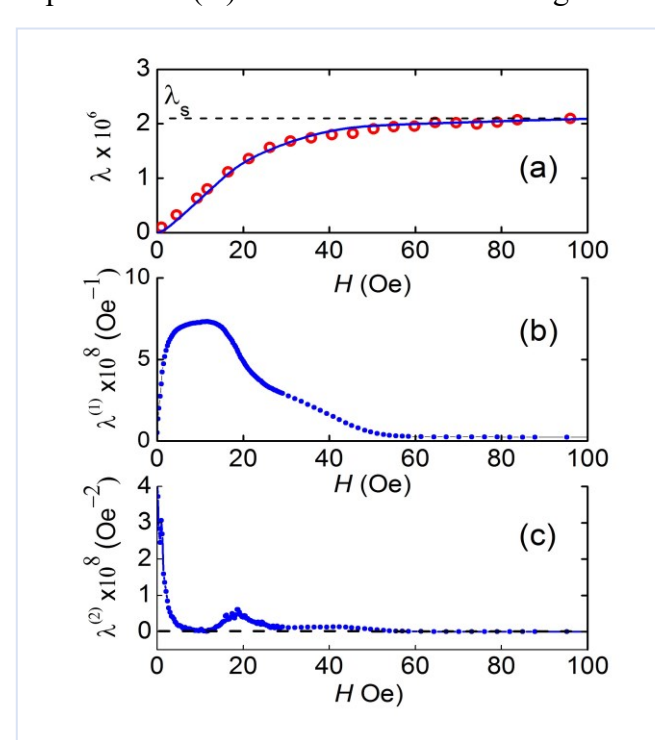


Fig. 12. YIG film characteristics versus magnetic field H: (a) magnetostriction λ , (b) linear piezomagnetic coefficient $\lambda^{(1)}$ and (c) nonlinear piezomagnetic coefficient $\lambda^{(2)}$. Data in (a) were measured with a strain gauge [27].

by dots in Fig. 12a. In the saturation field $H_S\approx80$ Oe, the magnitude of the YIG magnetostriction was $\lambda_S\approx2.1\cdot10^{-6}$, which agrees with the data of [28, 29]. Comparison of dependencies in Fig. 12a shows their good qualitative agreement. At the same time, in the curve showing the values found by the integration method, the number of points is much larger, and the measurement error is less than on the values measured by the tensometric method.

Figure 12b shows the field dependence of the linear piezomagnetic coefficient $\lambda^{(1)}(H) \sim u_1(H)$ for the YIG film, normalized by taking into account value of λ_s . The maximum value

of the coefficient $\max\{\lambda^{(1)}\}\approx 7.3\cdot 10^{-8}~\text{Oe}^{-1}$ is comparable to the piezomagnetic coefficient for Ni. The field $H_{\rm m}\approx 10~\text{Oe}$, at which the maximum is reached, is of the same order as the field for maximum piesomagnetic coefficient for Metglas [30].

For the linear converse ME effect, the ME coefficient can be estimated by the formula $\alpha_B = \delta B/e$ using the data in Fig. 8. We find the change in induction in the YIG film caused by the electric field using the Faraday law of electromagnetic induction $\delta B = v_1/(2\pi f_c SN)$, where f_c is the resonant frequency, N=60 is the number of turns of the measuring coil, the area S should be taken as the cross-sectional area of the YIG film $S = 1.5 \cdot 10^{-7}$ m², since the field is concentrated mainly inside the film. Substituting these values, we obtained $\delta B \approx 3.2 \cdot 10^{-3}$ T ≈ 32 G. Thus, the largest ME coefficient for the converse effect in the YIG film - quartz structure at H=10 Oe is $\alpha_B^{(1)} \approx 0.32$ G·cm/V. The resulting coefficient is an order of magnitude smaller than the coefficient for the converse ME effect of 5.5 G·cm/V in the Metglas-PZT structure [31] and is comparable to the coefficient of 0.27 G·cm/V for the Ni-PZT structure [32]. The $\lambda^{(1)}(H)$ field dependence is similar to the field dependence shown Fig. 8, which is consistent with the characteristics of the converse ME effect in heterostructures with layers of other magnetostrictive materials [31–33].

As shown earlier, nonlinear ME effects in FM-PE composite heterostructures arise mainly due to the nonlinearity of the FM layer of the structure; in the case of the direct ME effect due to the nonlinear dependence of the magnetostrictive deformation of the layer on the magnetic field $\lambda(H)$ [30], and in the case of the converse ME effect due to the nonlinear dependence of the magnetic induction of the layer on the deformation B(T) [31]. The nonlinearity of the piezoelectric effect in the PE layer and the acoustic nonlinearity of the layers at experimentally achievable amplitudes of ac electric field and strain do not make a significant contribution to the nonlinearity of the structure. With that, the measurements described above demonstrate that the magnitude of the nonlinear effects is significantly affected by the resonance conditions.

For the nonlinear direct ME effect, two options are realized. When the structure is excited by a magnetic field with a frequency $f_d/2$, the nonlinearity of magnetostriction leads to the generation of deformation at a doubled frequency f_d , which is equal to the frequency of the main acoustic resonance of the structure. The main resonance has a high quality factor $Q_d \approx 2 \cdot 10^3$. Due to the resonant increase in deformations, the PE layer generates an output voltage u_2 of large amplitude. When the structure is excited by a magnetic field with a frequency f_d , the nonlinearity of magnetostriction leads to the generation of a deformation with a frequency $2f_d$, which coincides with the resonant frequency of the second mode of longitudinal acoustic oscillations of the structure. However, the quality factor of this oscillation mode is much smaller (since the structure is

fixed in the center), which leads to the generation of low-amplitude voltage by PE layer. It is this ratio of amplitudes at different excitation frequencies that was observed in the experiment.

For the converse ME effect, two variants are also possible. When the structure is nonresonantly excited by an electric field with a frequency f/2, the PE layer generates a low-amplitude deformation and an ac induction with the same frequency. The nonlinearity of the inverse magnetostriction of the FM layer leads to the generation of induction with a doubled frequency, which is converted by the measuring coil into a low-amplitude output voltage. When the structure is excited by an electric field with a frequency fc equal to the frequency of the fundamental acoustic resonance of the structure, the deformation amplitudes increase by a factor of Qc, and a large-amplitude ac induction is generated in the FM layer.

For the direct ME effect upon excitation of the YIG-quartz structure by magnetic field with a frequency $f_d/2$, using the data in Fig. 5, the second harmonic generation efficiency can be estimated as $\alpha_E^{(2)} = u_2/(a_p h^2) \approx 0.73 \text{ V/(cm·Oe}^2)$. Thus, the nonlinear resonant ME coefficient for the YIG-quartz heterostructure is greater than the analogous coefficient $\alpha_E^{(2)} \approx 0.24 \text{ V/(cm·Oe}^2)$ for the Ni-PZT structure, but less than the coefficient $\alpha_E^{(2)} \approx 4.5 \text{ V/(cm·Oe}^2)$ for the Metglas-PZT structure [30]. When the composite was excited by a magnetic field at resonant frequency f_d , the second harmonic generation efficiency was $\alpha_E^{(2)} \approx 0.011 \text{ V/(cm·Oe}^2)$, i.e., by a factor of ~60 lower.

For the direct effect, the amplitude u_2 of the voltage harmonic with a doubled frequency is [25]

$$u_2(H) \approx K d_{31} \lambda^{(2)}(H) h^2$$
. (4)

Where $\lambda^{(2)} = \partial^2 \lambda / \partial H^2 |_H$ is the nonlinear piezomagnetic coefficient, h is the amplitude of the excitation field. Differentiating dependence $\lambda^{(1)}(H)$ in Fig. 12b, we obtain the field dependence $\lambda^{(2)}(H)$ shown in Fig.12c. For convenience of comparison with the experiment, the modulus of the nonlinear piezomagnetic coefficient is plotted along the vertical axis. It is seen, that the second harmonic amplitude should have a maximum in the absence of field $H \approx 0$, a maximum in the field range $H \sim 15-20$ Oe, and a broad and weak maximum in high fields. From a comparison of Fig. 12c and Fig.5 it can be seen, that the features of the field dependence of the YIG magnetostriction qualitatively well explain the shape of the field dependence of the second harmonic amplitude of ME voltage. We also note that the maximum value of the nonlinear piezomagnetic coefficient for the YIG film max $\{\lambda^{(2)}\} \approx 3 \cdot 10^{-8}$ Oe⁻² is comparable with the value of the nonlinear coefficient for Ni and permendur, but it is significantly less than the value of the coefficient for Metglas [30]. The quadratic dependence of the amplitude of the second harmonic of ME voltage on the amplitude of the excitation magnetic field h in Fig. 6 is also well described by (4).

For the converse nonlinear ME effect when the YIG-quartz structure is excited by an electric field with a frequency f_c , the second harmonic generation efficiency can be estimated using the formula $\alpha_B^{(2)} = \delta B_2 / e^2$, where δB_2 is the amplitude of the change in magnetic induction with a frequency of $2f_c$, caused by the electric field e. Using the law of electromagnetic induction and the data of Fig. 11, we obtain $\delta B = v_2 / (4\pi f_c SN) \approx 1.3$ G and a nonlinear ME coefficient of $\alpha_B^{(2)} \approx 1.3 \cdot 10^{-4}$ G·cm²/V². The obtained nonlinear ME coefficient is two orders of magnitude smaller than the nonlinear ME coefficient of $1.9 \cdot 10^{-2}$ G·cm²/V² for the Metglas-PZT structure [31]. The quadratic dependence of the voltage amplitude of the second harmonic v_2 on the amplitude of the excitation electric field e in Fig. 11 is well described by the theory [31].

To summarize, the resonant ME coefficient in heterostructures depends on the ratio of the thicknesses of the FM and PE layers and reaches a maximum at $a_{\rm m}/a_{\rm p} \sim 1$ [34]. For the investigated YIG film - quartz structure, the ratio of the layer thicknesses, taking into account the thickness of the GGG substrate, is $a_{\rm m}/(a_{\rm s}+a_{\rm p})\approx 0.04$. Therefore, it is expected that for the two-layer YIG film-quarz structures with thinner quartz layers ($a_{\rm m}\sim 50$ -100 µm), the ME coefficient can increase by an order of magnitude or more. For applications, the low conductivity of the YIG film is an advantage. This makes it possible to deposit conducting electrodes directly on the film surface, which opens the way to the fabrication of planar ME devices with coil-free excitation [35].

8. Conclusions

The nature of direct and converse ME effects was studied in a planar layered composite of a YIG film - quartz. The specific focus was on the linear and nonlinear ME effects at the longitudinal acoustic resonance mode when the structure was excited by a magnetic or electric field. At acoustic resonance frequency of the structure of ~128 kHz, a coefficient $\alpha_E^{(1)} \approx 8.8 \text{ V/(Oe cm)}$ for the direct linear ME effect, and coefficient $\alpha_B^{(1)} \approx 0.32 \text{ G/(V/cm)}$ for the converse linear ME effect were obtained. Nonlinear resonant ME effects of frequency doubling were observed: when the structure was excited by magnetic field at half the resonant frequency with an efficiency of $\alpha_E^{(2)} \approx 0.73 \text{ V/(cm·Oe}^2)$ and when the structure was excited by electric field at the resonant frequency, with an efficiency of $\alpha_B^{(2)} \approx 1.3 \cdot 10^{-4} \text{ G·cm}^2/\text{V}^2$. Nonlinear effects arise due to the nonlinearity of the YIG film magnetostriction. The results show that ME effects in the structure of the YIG film - quartz are comparable in magnitude with ME effects in similar structures with ferromagnetic layers of nickel, permendur, galphenol, have a high quality factor $Q \sim 2200$ and reach a maximum in low magnetic fields $H \sim 0.40$ Oe, as in structures with amorphous ferromagnets. This opens up prospects for use

of composites with YIG films to realize highly sensitive ME sensors of magnetic fields and various ME devices for microsystem engineering and electronics.

CRediT authorship contribution statement

D.A. Burdin: Conceptualization, Investigation. **D.V. Chashin**: Visualization, Metodology. **N.A. Ekonomov**: Supervision, Resources, Investigation. **P. Zhou**: Visualization, Metodology. **G. Srinivasan**: Writing – review and editing, Investigation. **Y.K. Fetisov**: Writing – original draft, Project administration.

Declaration of Competing Interest

The authors declare that they have no known competing financial interests or personal relationship that could have appeared to influence the work reported in this paper.

Acknowledgements:

Experimental investigations at RTU MIREA was supported by the Russian Science Foundation, project No. 22-29-01093. Some measurements were carried out on the equipment of the Joint Center for Common Use of RTU MIREA. Theoretical research at Oakland University was supported by grants from the National Science Foundation (DMR-1808892, ECCS-1923732) and the Air Force Office of Scientific Research (AFOSR), Award No. FA9550-20-1-0114.

References

- 1. C.-W. Nan, M.I. Bichurin, S. Dong, D. Viehland, G. Srinivasan, Multiferroic magnetoelectric composites: Historical perspective, status, and future directions, J. Appl. Phys. 103(3) (2008) 31101. doi:10.1063/1.2836410
- 2. J. van Suchtelen, Product Properties: A New Application of Composite Materials. Philips Res. Repts., **27**, 28-37 (1972).
- 3. D.R. Patil, A. Kumar, J. Ryu, Recent progress in devices based on magnetoelectric composite thin films, *Sensors*, 21(23) (2021) 8012. https://doi.org/10.3390/s21238012\
- 4. A.R. Will-Cole, A.E. Hassanien, S.D. Calisgan et al, Tutorial: piezoelectric and magnetoelectric N/MEMS materials, devices, and applications, J. Appl. Phys., 131 (2022) 241101. https://doi.org/10.1063/5.0094364
- 5. N. Pereira, A.C. Lima, S. Lanceros-Mendez, P. Martins, Magnetoelectrics: Three Centuries of Research Heading Towards the 4.0 Industrial Revolution. Materials, 13(18) (2020) 4033. doi:10.3390/ma13184033
- 6. X. Liang, C. Dong, H. Chen et al. A Review of Thin-Film Magnetoelastic Materials for Magnetoelectric Applications. Sensors, 20(5) (2020) 1532. doi:10.3390/s20051532
- 7. M.I. Bichurin, D.A. Filippov, V.M. Petrov, V.M. Laletsin, N. Paddubnaya, G. Srinivasan Resonance magnetoelectric effects in layered magnetostrictive-piezoelectric composites, Phys. Rev. B 68 (2003) 132408. https://dx.doi.org/10.1103/PhysRevB.68.132408

- 8. I.V. Zavislyak and M. A. Popov, Microwave properties and applications of yttrium iron garnet (YIG) films: current state of art and perspectives, In Yttrium: Compounds, Production and Applications. Editors: Bradley D. Volkerts, Nova Science Publishers, Inc., pp. 87-125, 2009.
- 9. G. Schmidt, C. Hauser, P. Trempler, M. Paleschke, E. Papaioannou, Ultra thin films of yttrium iron garnet with very low damping: A review, Phys. Stat. Sol.. 57 (2020) 1900644. doi:10.1002/pssb.201900644
- 10. Y. Rao, H. Zhang, Q. Yang, et al, Liquid phase epitaxy magnetic garnet films and their applications. Chin. Phys. B, 27(8) (2018) 086701. doi:10.1088/1674-1056/27/8/086701
- 11. T. H. O'Dell, An induced magneto-electric effect in yttrium iron garnet, The Philosophical Magazine: A Journal of Theoretical Experimental and Applied Physics, 16:141 (1967) 487-494, DOI: 10.1080/14786436708220859
- 12. G. Velleaud, B. Sangare, M. Mercier, G. Aubert (1984). Magnetoelectric properties of Yttrium Iron Garnet, 52(1) (1984) 71–74. doi:10.1016/0038-1098(84)90721-x
- 13. F. Chen, Z. Zhang, X. Wang, J. Ouyang, X. Feng, Z. Su, Y. Chen, V. Harris. Room temperature magnetoelectric effect of YFeO₃–Y₃Fe₅O₁₂ ferrite composites. J. Alloys & Comp., 656 (2016) 465–469. doi:10.1016/j.jallcom.2015.09.268
- 14. I.V. Lisnevskaya, I.A. Aleksandrova, Magnetoelectric composites of lead-free piezoelectrics and yttrium iron garnet: interfacial reactions and functional properties. Appl. Phys. A 126 (2020) 406. https://doi.org/10.1007/s00339-020-03602-6
- 15. J. Lian, F. Ponchel, N. Tiercelin et al. Electric field tuning of magnetism in heterostructure of yttrium iron garnet film/lead magnesium niobate-lead zirconate titanate ceramic. Appl. Phys. Lett., 112(16) (2018) 162904. doi:10.1063/1.5023885
- S. Shastry, G. Srinivasan, M.I. Bichurin, V.M. Petrov, A.S. Tatarenko, Microwave magnetoelectric effects in single crystal bilayers of yttrium iron garnet and lead magnesium niobate-lead titanate. Phys. Rev. B, 70(6) (2004) 064416. doi:10.1103/PhysRevB.70.064416
- 17. S. Alekseev, N. Polzikova, I. Kotelyanskii, Y. Fetisov, Tunable HBAR based on magnetoelectric YIG/ZnO structure. 2012 IEEE International Ultrasonics Symposium Dresden, Germany, 2481–2484. doi:10.1109/ultsym.2012.0621
- 18. G. Srinivasan; C. P. De Vreugd; M. I. Bichurin; V. M. Petrov. Magnetoelectric interactions in bilayers of yttrium iron garnet and lead magnesium niobate-lead titanate: Evidence for strong coupling in single crystals and epitaxial films. Appl. Phys. Lett., 86 (2005) 222506. doi:10.1063/1.1943491
- 19. G. Sreenivasulu, V.M. Petrov, L.Y. Fetisov, Y.K. Fetisov, G. Srinivasan, Magnetoelectric interactions in layered composites of piezoelectric quartz and magnetostrictive alloys. Phys. Rev. B, 86(21) (2012) 214405. doi:10.1103/physrevb.86.214405.
- 20. G. Srinivasan, C.P. De Vreugd, V.M. Laletin, N. Paddubnaya, M.I. Bichurin, V.M. Petrov, D.A. Filippov, Resonant magnetoelectric coupling in trilayers of ferromagnetic alloys and piezoelectric lead zirconate titanate: The influence of bias magnetic field. Phys. Rev. B, 71(18) (2005) 184423. doi:10.1103/physrevb.71.184423
- 21. S. Timoshenko, *Vibration Problems in Engineering*, D. Van Nostrand Company Inc., Toronto, 1955, p. 310.
- 22. G. Sreenivasulu, L.Y. Fetisov, Y.K. Fetisov, G. Srinivasan, Piezoelectric single crystal langatate and ferromagnetic composites: Studies on low-frequency and resonance magnetoelectric effect, Appl. Phys. Lett. 100 (2012) 052901. https://dx.doi.org/10.1063/1.3679661
- 23. C. Kirchhof, M. Krantz, I. Teliban et al, Giant magnetoelectric effect in vacuum. Appl. Phys. Lett., 102(23) (2013) 232905. doi:10.1063/1.4810750
- 24. F.A. Fedulov, D.V. Saveliev, D.V. Chashin, V.I. Shishkin, Y.K. Fetisov. Magnetoelectric effects in stripe- and periodic heterostructures based on nickel–lead zirconate titanate bilayers. Rus. Techn. J. 10(3) (2022) 64. https://doi.org/10.32362/2500-316X-2022-10-3-64-73

- 25. L.Y. Fetisov, D.A. Burdin, N.A. Ekonomov, D.V. Chashin, J. Zhang, G. Srinivasan, Y.K. Fetisov. Nonlinear magnetoelectric effects at high magnetic field amplitudes in composite multiferroics, J. Phys. D: Appl. Phys., (2018) 154003. DOI: 10.1088/1361-6463/aab384
- 26. D. A. Filippov, V. M. Laletin, N. N. Poddubnaya et al. Magnetostriction via magnetoelectricity: using magnetoelectric response to determine the magnetostriction characteristics of composite multiferroics. Techn. Phys. Lett., 45 (2019) 1152–1154. doi:10.1134/S1063785019110208
- 27. D.V. Chashin, D.A. Burdin, L.Y. Fetisov, N.A. Ekonomov, Y.K. Fetisov, Precise measurements of magnetostriction of ferromagnetic plates, J. Siberian Federal Univ. Math. & Phys. 11 (2018) 30-34. DOI: 10.17516/1997-1397-2018-11-1-30-34.
- 28. A. Nakamura, Y. Sugiura, Magnetostriction of yttrium iron garnet, J. Phys. Soc. Jap., 15 (1960) 1704.
- 29. A.B. Smith, R.V. Jones, Magnetostriction constants from ferromagnetic resonance, J. Appl. Phys., 34(4) (1963) 1283-1284.
- 30. D.A Burdin, D.V. Chashin, N.A. Ekonomov, L.Y. Fetisov, Y.K. Fetisov, G. Sreenivasulu, G. Srinivasan, Nonlinear magneto-electric effects in ferromagnetic-piezoelectric composites. J. Mag. Magn. Mater., 358-359 (2014) 98–104. doi:10.1016/j.jmmm.2014.01.062
- 31. L.Y. Fetisov, D.V. Chashin, D.A. Burdin, D.V. Saveliev, N.A. Ekonomov, G. Srinivasan, Y.K. Fetisov, Nonlinear converse magnetoelectric effects in a ferromagnetic-piezoelectric bilayer. Appl. Phys. Lett. 113(21) (2018) 212903. doi:10.1063/1.5054584
- 32 Y. K. Fetisov, V. M. Petrov, and G. Srinivasan, Inverse magnetoelectric effects in a ferromagnetic–piezoelectric layered structure, J. Mater. Res. 22 (2007) 2074. doi 10.1557/JMR.2007.0262
- 33 Y.K. Fetisov, K.E. Kamentsev, D.V. Chashin, L.Y. Fetisov, G. Srinivasan, Converse magnetoelectric effect in a galfenol and lead zirconate titanate bilayer, J. Appl. Phys., 105 (2009) 123918. DOI: 10.1063/1.3152953
- 34. M.I. Bichurin, V.M. Petrov, G. Srinivasan, Theory of low-frequency magnetoelectric coupling in magnetostrictive-piezoelectric bilayers. Phys. Rev. B, 68(5) (2003) 054402. doi:10.1103/PhysRevB.68.054402
- 35. D. Burdin, D. Chashin, L. Fetisov, D. Saveliev, N. Ekonomov, M. Vopson, Y. Fetisov, Towards fabrication of planar magnetoelectric devices: coil-free excitation of magnetostrictive-piezoelectric heterostructures, Actuators, (2021) 294. doi.org/10.3390/act10110294